

# Design and processor-in-the-loop implementation of Backstepping Integrator Control for a multi-drive web winding system

Mounir Bensaïd\* , Abdellfattah Ba-Razzouk , Mustapha Elharoussi , and Mohammed El Haïssouf 

Laboratory of Mathematics, Computer and Engineering Sciences Laboratory (MISI), Team: Systems Analysis and Information (ASTI). FST Settat. Hassan First University of Settat University Complex, Km 3, Casablanca Road, P.O. Box 577, Settat 26000, Kingdom of Morocco

Received: 13 April 2025 / Accepted: 28 January 2026

**Abstract.** This work presents a nonlinear control approach specifically tailored for a Multi-Drive Web Winding System (MDWWS), utilizing the Integral Backstepping Control (IBSC) technique. The proposed strategy is designed to improve the precision of both speed control and mechanical tension regulation across multiple coordinated drives. A detailed formulation of the control law is provided, grounded in the Backstepping framework and extended with integral action to enhance steady-state performance. The theoretical foundations of the IBSC method are thoroughly discussed, and its performance is benchmarked against the conventional Proportional-Integral (PI) controller. The comparative study focuses on evaluating the robustness and adaptability of each control method in the presence of system parameter variations and external disturbances. To validate the effectiveness of the proposed control strategy, a Processor-in-the-Loop (PIL) setup is implemented, integrating automatic code generation with hybrid simulation. This platform enables real-time execution of the control algorithm on the TMDSCNCD28379D DSP board while emulating the dynamic behavior of the web winding system in Simulink, thus providing a realistic and efficient environment for performance evaluation.

**Keywords:** Multi-Drive Web winding system, Integral Backstepping control, PIL, DSP TMDSCNCD28379D.

## 1 Introduction

Nowadays, industry is shifting toward advanced and sophisticated electric drive systems, increasingly adopting multi-machine, multi-converter configurations to meet growing and specific industrial needs [1, 2]. In the past, drive systems were relatively simple, typically consisting of an electric motor connected to a frequency converter. While this setup was effective for basic speed and torque control in certain applications, it was often bulky in terms of volume [3]. In this context, Multi-Drive Web Winding System (MDWWS) have emerged. These systems consist of multiple electric motors, each driven by a voltage inverter, all connected to a common DC bus [2]. Multi-Motor System has become widespread in industries that naturally require distributed actuators, such as the paper, plastic [1], textile [4], and metalworking industries [5], among others. They are specifically designed to meet the needs of these sectors in terms of speed control, mechanical tension, torque regulation, and the handling of rolled/unrolled materials.

The main objective of the control system in web handling processes is to maintain continuous production by preventing web breaks, folds, or damage. Significant fluctuations in speed or mechanical tension can cause premature wear or even complete loss of the web. To address this, the control system must ensure accurate regulation of both speed and tension, with effective decoupling to avoid undesirable interactions between them. Additionally, it must demonstrate robustness to mechanical variations, such as changes in the inertia of the unwinding/rewinding units and in the web's Young's modulus. Fulfilling these requirements is crucial to maintaining the quality and reliability of the industrial process.

Many industrial web transport systems have employed decentralized PI controllers [6]. A comprehensive review of web tension control challenges can be found in [7]. Alternative control approaches have also been explored, including fuzzy logic [8, 9], neural networks [10], optimal control [11], nonlinear sliding mode control [12, 13], Active Disturbance Rejection Control (ADRC) [14, 15], and robust control methods [16]. Robust feedback control based on Lyapunov theory [17] and multivariable  $H_\infty$  controllers have also been proposed for web handling systems [18].

\* Corresponding author: [mo.bensaid@uhp.ac.ma](mailto:mo.bensaid@uhp.ac.ma)

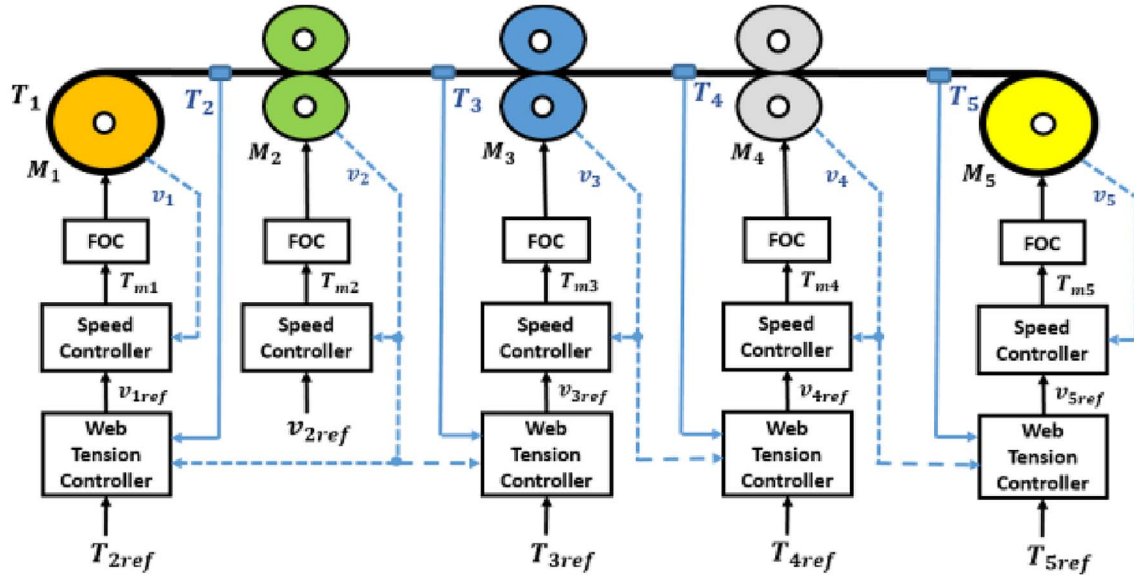


**Figure 1.** Backstepping control structure applied to the MDWWS.

Among the most prominent nonlinear control design techniques is the Backstepping approach. Adaptive Backstepping control aims to achieve precise coordination between motors while compensating for load variations and external disturbances. This nonlinear strategy is grounded in feedback principles, allowing dynamic adjustment of system parameters to ensure optimal performance [19].

In this study, our contribution focuses on improving the system's robustness to parametric variations in the Young's modulus and the total inertias of the winder and unwinder by designing a nonlinear controller based on the integral Backstepping approach. This method is intended to simultaneously control the web's scrolling speed and mechanical tension within the system under study, as shown in Figure 1.

The validation of control strategies within a Model-Based Design (MBD) framework is carried out using Processor-in-the-Loop (PIL) simulation to assess the performance of controllers on a MDWWS model [20, 21]. This hybrid simulation technique is especially effective for rapid prototyping. In this setup, the system model runs in Simulink, while control and observation algorithms are executed in real time on the TMDSCNCD28379D DSP board (see Fig. 2). This configuration offers a realistic and efficient environment to evaluate control performance under near-real-world conditions before implementation on the physical system.

The structure of this paper is organized to provide a clear and progressive understanding of the proposed approach. Section 2 presents the dynamic modeling of the web winding system, with particular emphasis on the mechanical coupling between the multiple motors and the web material. In Section 3, the design and formulation of the nonlinear control strategy based on the integral Backstepping technique are detailed, targeting precise regulation of both mechanical tension and transport speed. Section 4 showcases the simulation results conducted in MATLAB/

Simulink, including a Processor-in-the-Loop (PIL) implementation, to evaluate the controller's performance under various operating scenarios. Lastly, Section 5 summarizes the key findings and concludes the study, highlighting potential avenues for future work.

## 2 Mathematical Modeling of the Web Winding System

Figure 3 illustrates a basic multi-motor web transport setup, typically found in winder systems, featuring two motors:  $M_1$  for unwinding and  $M_2$  for winding. The modeling of these systems is based on three core principles: Hooke's law, Coulomb's law, and the law of mass conservation, which together enable the calculation of web tension between the two rolls [22–24].

Equation (1) defines the web tension  $T_2$  as a function of the web length  $L$  and the linear speeds of motors  $V_1$  and  $V_2$ .

$$L \frac{dT_2}{dt} \cong ES(V_2 - V_1) + T_1 V_1 - T_2(2V_1 - V_2). \quad (1)$$

The Multi-Drive Web Winding System under analysis comprises five motors, and its dynamic behavior, specifically motor speeds and web tension, is characterized by the following set of equations:

$$\frac{d(J_k(t)\Omega_k)}{dt} = T_{mk} - T_{res-k} - f_k(t)\Omega_k, \quad (2)$$

$$L_{k+1} \frac{dT_{k+1}}{dt} = ES(V_{k+1} - V_k) + T_k V_k - T_{k+1} V_{k+1}. \quad (3)$$

For  $k = 1$  to 5, the expressions  $V_k = R_k \Omega_k$  and  $T_{res-k} = R_k (T_k - T_{k+1})$  represent the linear web speed and the load

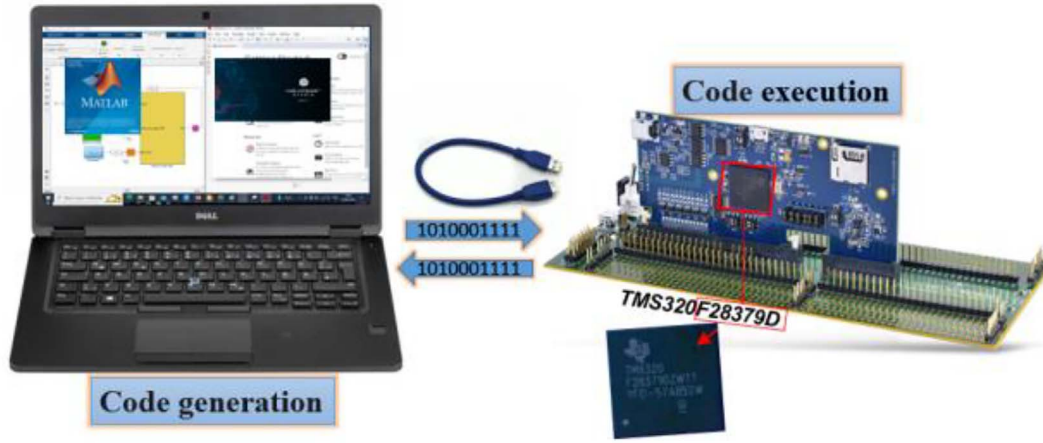


**Figure 2.** Operation of the hybrid Processor-in-the-Loop (PIL) platform.

torque disturbance, respectively, where  $\Omega_k$  is the rotational speed and  $R_k$  denotes the roll radius.

By reformulating equations (2) and (3), the state-space representation of the Multi-Drive Web Winding System is obtained as follows:

$$\dot{X} = AS - B - CX, \quad (4)$$

where:

$$S = \begin{bmatrix} V_2 \\ V_3 \\ V_4 \\ V_5 \\ T_{m1} \\ T_{m2} \\ T_{m3} \\ T_{m4} \\ T_{m5} \end{bmatrix}, \quad X = \begin{bmatrix} T_2 \\ T_3 \\ T_4 \\ T_5 \\ \Omega_1 \\ \Omega_2 \\ \Omega_3 \\ \Omega_4 \\ \Omega_5 \end{bmatrix},$$

$$B = \begin{bmatrix} V_1(ES - T_1) \\ V_2(ES - T_2) \\ V_3(ES - T_3) \\ V_4(ES - T_4) \\ \frac{R_1}{J_1}(T_1 - T_2) \\ \frac{R_2}{J_2}(T_2 - T_3) \\ \frac{R_3}{J_3}(T_3 - T_4) \\ \frac{R_4}{J_4}(T_4 - T_5) \\ \frac{R_5}{J_5}(T_5 - T_s) \end{bmatrix},$$

$$A = \begin{bmatrix} \frac{ES}{L_2} & 0 & 0 & 0 & 0 & 0 & 0 & 0 & 0 \\ 0 & \frac{ES}{L_2} & 0 & 0 & 0 & 0 & 0 & 0 & 0 \\ 0 & 0 & \frac{ES}{L_2} & 0 & 0 & 0 & 0 & 0 & 0 \\ 0 & 0 & 0 & \frac{ES}{L_2} & 0 & 0 & 0 & 0 & 0 \\ 0 & 0 & 0 & 0 & \frac{1}{J_1} & 0 & 0 & 0 & 0 \\ 0 & 0 & 0 & 0 & 0 & \frac{1}{J_2} & 0 & 0 & 0 \\ 0 & 0 & 0 & 0 & 0 & 0 & \frac{1}{J_3} & 0 & 0 \\ 0 & 0 & 0 & 0 & 0 & 0 & 0 & \frac{1}{J_4} & 0 \\ 0 & 0 & 0 & 0 & 0 & 0 & 0 & 0 & \frac{1}{J_5} \end{bmatrix},$$

$$C = \begin{bmatrix} V_2 & 0 & 0 & 0 & 0 & 0 & 0 & 0 & 0 \\ 0 & V_3 & 0 & 0 & 0 & 0 & 0 & 0 & 0 \\ 0 & 0 & V_4 & 0 & 0 & 0 & 0 & 0 & 0 \\ 0 & 0 & 0 & V_5 & 0 & 0 & 0 & 0 & 0 \\ 0 & 0 & 0 & 0 & \frac{f_1}{J_1} & 0 & 0 & 0 & 0 \\ 0 & 0 & 0 & 0 & 0 & \frac{f_2}{J_2} & 0 & 0 & 0 \\ 0 & 0 & 0 & 0 & 0 & 0 & \frac{f_3}{J_3} & 0 & 0 \\ 0 & 0 & 0 & 0 & 0 & 0 & 0 & \frac{f_4}{J_4} & 0 \\ 0 & 0 & 0 & 0 & 0 & 0 & 0 & 0 & \frac{f_5}{J_5} \end{bmatrix}.$$

Matrices  $A$  and  $C$  are square and diagonal matrices of size  $n \times n$ . The matrix  $B \in R^n$  represents the control input. The state vector  $X \in R^n$  characterizes the system dynamics, while the vector  $S \in R^n$  includes the torque and speed components of each motor.

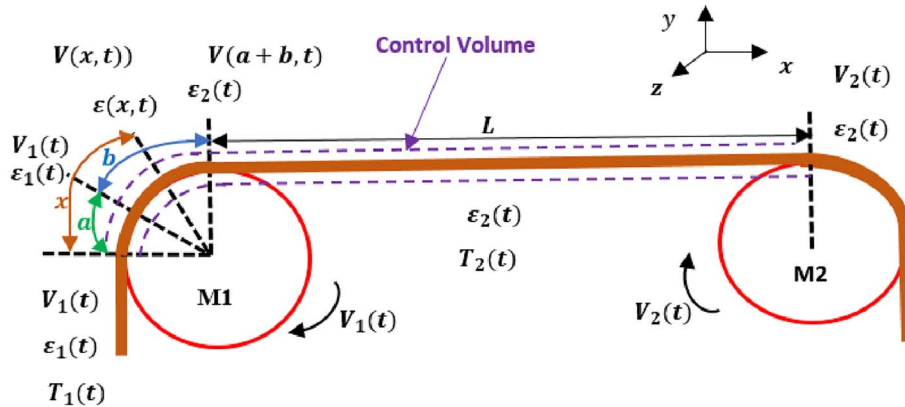


Figure 3. Web Tension in Roll Handling.

### 3 Design of the control law for the MDWWS using Integral Backstepping

The primary objective of applying the Backstepping method is to achieve asymptotic convergence of the vector  $\gamma$  towards a bounded reference vector  $\gamma_{\text{ref}}$ , where  $X = \frac{d\gamma}{dt}$ . The set of internal signals is utilized within the context of the closed-loop system [25–27].

Initially, the first step consists of defining the error between  $\gamma$  and  $\gamma_{\text{ref}}$ .

$$\varepsilon_\gamma = \gamma_{\text{ref}} - \gamma. \quad (5)$$

The dynamics of which can be expressed as follows:

$$\dot{\varepsilon}_\gamma = \dot{\gamma}_{\text{ref}} - X. \quad (6)$$

This definition outlines our control objective, which is to drive the error  $\varepsilon_\gamma$  to asymptotically converge to zero. This goal will be accomplished through our incremental design approach. In fact, the convergence rate of the error  $\varepsilon_\gamma$  can be controlled by incorporating the integration of  $\varepsilon_\gamma$  as follows:

$$\varepsilon_I = \int_0^t \varepsilon_\gamma(\tau) d\tau. \quad (7)$$

We will now extend the system to the subsystem  $(\Delta_1)$  (8). The state representation then becomes:

$$\Delta_1 \begin{cases} \dot{\varepsilon}_i = \varepsilon_\gamma \\ \dot{\varepsilon}_\gamma = \dot{\gamma}_{\text{ref}} - X \end{cases}. \quad (8)$$

The first Lyapunov function is chosen in the following format:

$$V_1 = \frac{K_I}{2} \varepsilon_I^2 + \frac{1}{2} \varepsilon_\gamma^2, \quad (9)$$

where  $K_I$  is a positive constant that adjusts the value of the integral to be incorporated into the system dynamics.

We now choose the virtual control law  $X$  so that the derivative of  $V_1$ , denoted  $\dot{V}_1$ , is less than or equal to 0. According to Lyapunov stability theory, it is known that such a control law stabilizes the first subsystem  $(\Delta_1)$ .

We now define the virtual control law  $X$  such that the derivative of  $V_1$ , denoted  $\dot{V}_1$ , is less than or equal to zero. According to Lyapunov stability theory, this control law ensures the stabilization of the first subsystem  $(\Delta_1)$ .

Now, considering:

$$X = K_\gamma \varepsilon_\gamma + \dot{\gamma}_{\text{ref}} + K_I \varepsilon_I. \quad (10)$$

The derivative of the Lyapunov control function is then given by:

$$\dot{V}_1 = -K_\gamma \varepsilon_\gamma^2. \quad (11)$$

Now, we can consider  $X$  in (10) as a reference ( $X_{\text{ref}}$ ) for the next design step.

Next, we proceed to the following step, which focuses on ensuring that the signals  $X$  track their reference  $X_{\text{ref}}$ . To accomplish this, we can derive the dynamics of the error between the vectors  $X$  and  $X_{\text{ref}}$  as follows:

$$\dot{\varepsilon}_{V-T} = K_\gamma (\dot{\gamma}_{\text{ref}} - X) + \ddot{\gamma}_{\text{ref}} + K_I \varepsilon_\gamma - AS + B + CX, \quad (12)$$

where  $\varepsilon_{V-T}$  corresponds to  $X_{\text{ref}} - X$ , representing the error vector of the motor speeds and the tensions in the web.

Now, let's extend once again the last subsystem  $(\Delta_2)$ , which is described by the following equations:

$$\Delta_2 \begin{cases} \dot{\varepsilon}_i = \varepsilon_\gamma \\ \dot{\varepsilon}_\gamma = -K_p \varepsilon_\gamma - K_I \varepsilon_I + \varepsilon_{V-T} \\ \dot{\varepsilon}_{V-T} = K_\gamma (\dot{\gamma}_{\text{ref}} - X) + \ddot{\gamma}_{\text{ref}} + K_I \varepsilon_\gamma - AS \\ \quad + B + CX \end{cases}. \quad (13)$$

By introducing  $S$  as a virtual control input, the overall system can be stabilized using the Lyapunov function  $V_2$ .

$$V_2 = \frac{K_I}{2} \varepsilon_I^2 + \frac{1}{2} \varepsilon_\gamma^2 + \frac{1}{2} \varepsilon_{V-T}^2. \quad (14)$$

Whose time derivative of  $V_2$  is:

$$\begin{aligned} \dot{V}_2 = & -K_\gamma \varepsilon_\gamma^2 + \varepsilon_{V-T} \{ \varepsilon_\gamma + K_\gamma (-K_\gamma \varepsilon_\gamma - K_I \varepsilon_I + \varepsilon_{V-T}) \\ & + \ddot{\gamma}_{\text{ref}} + K_I \varepsilon_\gamma - AS + B + CX \}. \end{aligned} \quad (15)$$

We select the virtual stabilization control law to ensure that  $\dot{V}_2$  is negative. Assuming all parameters in the

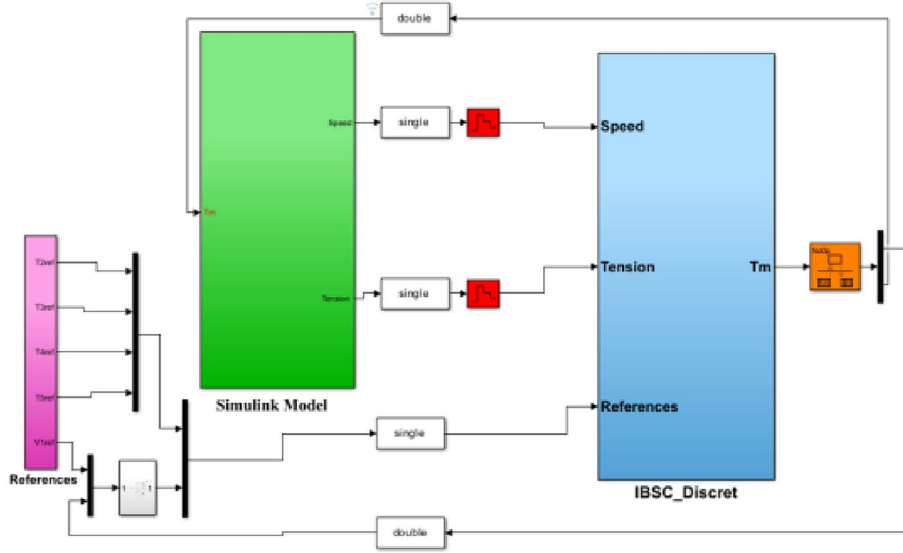


**Figure 4.** Discrete implementation of backstepping integrator control in simulink.

matrices  $A$ ,  $B$ , and  $C$  are known, the control law  $S$  that stabilizes the entire system is as follows:

$$\begin{aligned} S &= A^{-1}\{K_V\varepsilon_{V-T} + \varepsilon_\gamma + K_\gamma(-K_\gamma\varepsilon_\gamma - K_I\varepsilon_I + \varepsilon_{V-T}) \\ &+ \ddot{\gamma}_{ref} + K_I\varepsilon_\gamma + B + CX\} = A^{-1}\{(1 - K_\gamma^2 + K_I)\varepsilon_\gamma \\ &+ (K_\gamma + K_V)\varepsilon_{V-T} - K_\gamma K_I\varepsilon_I + \ddot{\gamma}_{ref} + B + CX\}. \end{aligned} \quad (16)$$

The time derivative of the Lyapunov function  $V_2$  becomes:

$$\dot{V}_2 = -K_\gamma\varepsilon_\gamma^2 - K_V\varepsilon_{V-T}^2, \quad (17)$$

where  $K_\gamma > 0$  and  $K_V > 0$  are tuning parameters. As a result, the virtual control law  $S$  stabilizes the last subsystem ( $\Delta_2$ ) since the time derivative  $\dot{V}_2$  is semi-negative along its trajectories, ensuring the convergence of the error  $\varepsilon_{V-T}$ .

Since the parameter matrices  $A$ ,  $B$ , and  $C$  are unknown, we use their estimates, denoted  $\hat{A}$ ,  $\hat{B}$  and  $\hat{C}$  [28]. We choose to implement an indirect adaptive control law as follows:

$$\begin{aligned} U &= \hat{A}^{-1}\left\{(1 - K_\gamma^2 + K_I)\varepsilon_\gamma + (K_\gamma + K_V) \right. \\ &\left. \varepsilon_{V-T} - K_\gamma K_I\varepsilon_I + \ddot{\gamma}_{ref} + \hat{B} + \hat{C}X\right\}. \end{aligned} \quad (18)$$

The adaptation law for the matrices is given by:

$$\begin{cases} \dot{\hat{A}}^{-1} = \delta_1\varepsilon_{V-T} \begin{bmatrix} (1 - K_\gamma^2 + K_I)\varepsilon_\gamma + \\ (K_\gamma + K_V)\varepsilon_{V-T} \\ -K_\gamma K_I\varepsilon_I + \ddot{\gamma}_{ref} \\ +\hat{B} + \hat{C}X \end{bmatrix} \\ \dot{\hat{B}} = \delta_2\varepsilon_{V-T} \\ \dot{\hat{C}} = \delta_3\varepsilon_{V-T}X \end{cases} \quad (19)$$

## 4 Validation of Backstepping Integrator Control through the PIL technique

In our PIL application, we utilize the integrated MATLAB/Simulink environment, covering the design, code generation, and PIL co-simulation with the TMDSCNCD28379D development kit for the C2000™ Delfino MCU controlCARD™. The following sections will describe the development environment, the code generation process, and the co-simulation steps.

The IBSC (Integrator Backstepping Control) discussed earlier is implemented in discrete mode within Simulink, integrated into the “IBSC\_Discret” block, as shown in Figure 4. The continuous mode applies to the multi-motor system model. The two modes are separated by sample-and-hold blocks with a sampling period of  $T_e = 200 \mu\text{s}$  and simulation step-size adaptation blocks.

After testing the setup in the Simulink simulator, the “IBSC\_Discret” block is converted into a subsystem for automatic code generation in C or C<sup>++</sup>. This generates a new block, “IBSC\_PIL,” with “PIL” added in the middle of its name. This block is then integrated into the simulation environment and prepared for validation using the “Processor-In-the-Loop” (PIL) technique, as shown in Figure 5.

The test setup, shown in Figure 6, involves generating code based on the IBSC model, compiling it, and executing it on the TMDSCNCD28379D target. The goal is to validate the generated code by comparing its results with those from the Simulink model. In this PIL configuration, the speed and mechanical tension values calculated in Simulink are sent as inputs to the IBSC\_PIL algorithm running on the F28379D DSP. The PIL block in Simulink serves as an interface, transmitting inputs to the DSP, while the control algorithm outputs are returned to the Simulink model via USB serial communication. To validate the effectiveness of the proposed integrator Backstepping control, we also implemented a control system using standard PI controllers

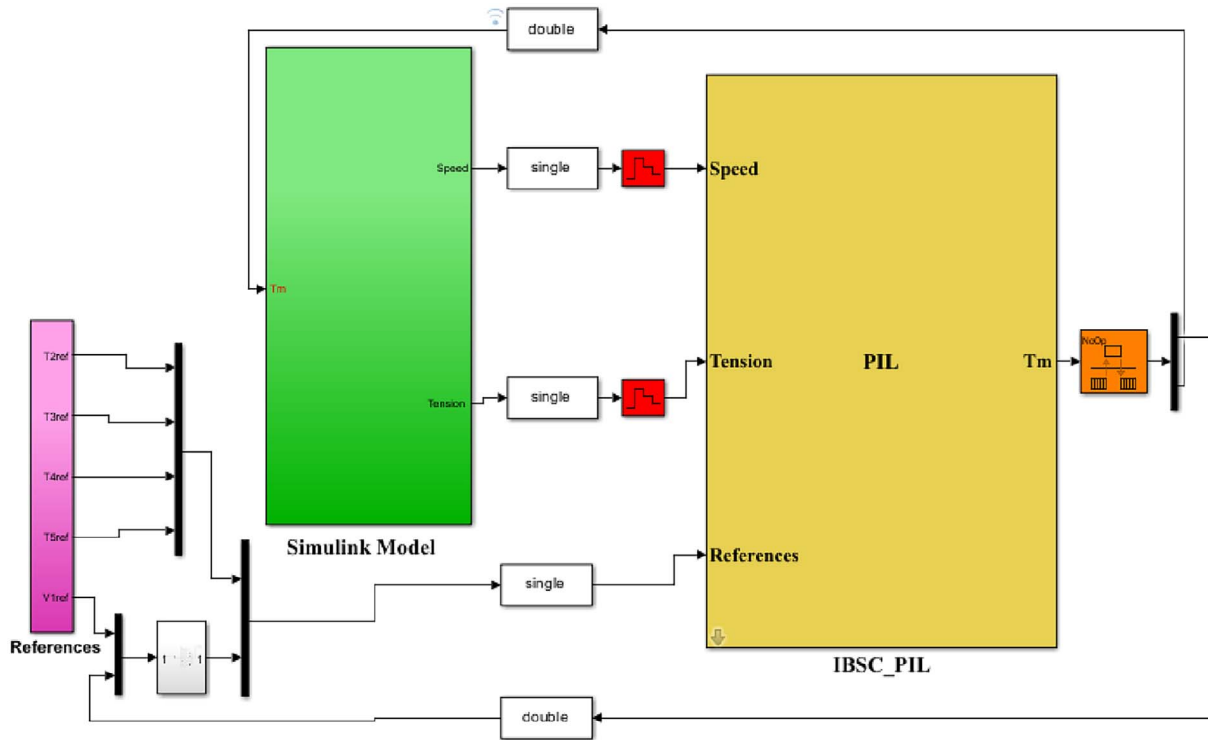


Figure 5. Code and PIL block generation in simulink.

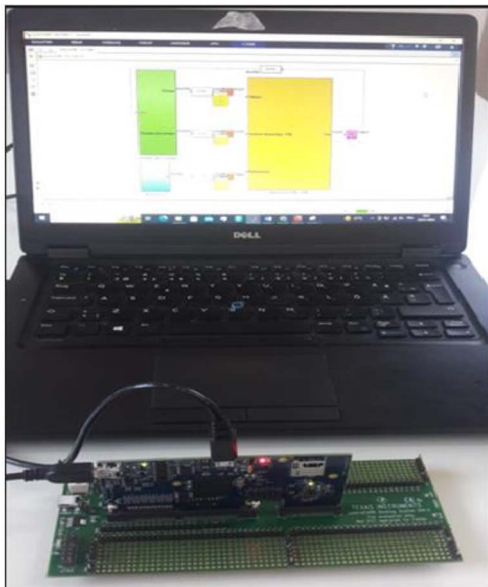


Figure 6. Test setup for PIL co-simulation.

for comparison. This comparison was performed under the following conditions:

- All parameters are perfectly known.
- The Young's modulus  $E$  is underestimated by a factor of 2 in the controller.
- The total inertias  $J_1$  and  $J_5$ , as perceived by the motors  $M_1$  and  $M_5$ , respectively, are overestimated by a factor of 2.

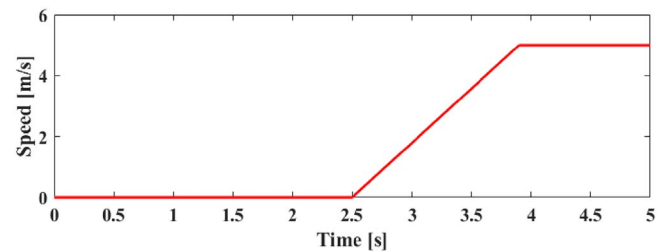


Figure 7. Reference linear speed for master motor  $M_2$ .

Reference signals for mechanical tension are applied progressively to different sections of the web, starting from the last and moving towards the first. A filtered speed ramp is then applied to the web, as shown in Figures 6 and 7. The winder system and control parameters used in the simulations are detailed in Appendix A.

In the analysis of the results shown in Figure 8, we observe that the tensions of the last four motors ( $T_2$ ,  $T_3$ ,  $T_4$ ,  $T_5$ ) quickly converge to their setpoint values, represented by 4 N steps. Examining the results for the tensions and speeds (Figs. 9 and 10) of these motors, we find that the steady-state errors are also zero. However, oscillations appear in the mechanical tensions during the transient state. These oscillations can be attributed to the increased order of the subsystems, the use of derivatives in the controller, and the couplings between the control loops, demonstrating the challenges associated with the system's increasing complexity.

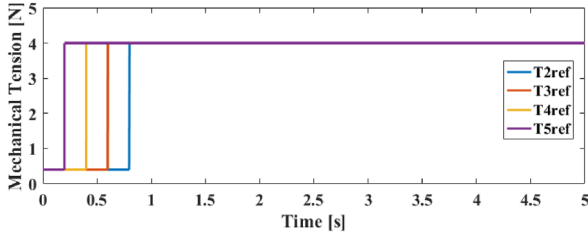


Figure 8. Mechanical tension references.

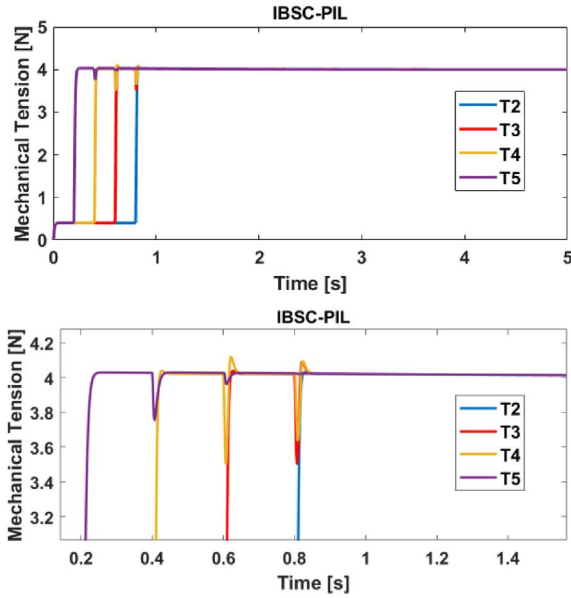


Figure 9. Responses of mechanical tensions by PIL.

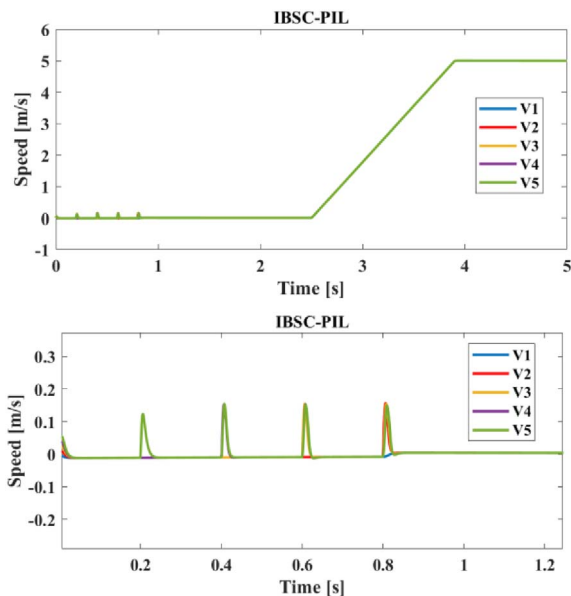


Figure 10. Response speeds of the five motors by PIL.

**Table 1.** Performance indices (ISE) for mechanical tension  $\Delta T_2$ ,  $\Delta T_3$ ,  $\Delta T_4$  and  $\Delta T_5$ , for exact parameters and underestimation of (E),  $J_1$ , and  $J_5$  between [0–1]s.

		PI	IBSC
Exact parameters	$\Delta T_2$	0.007	0,07
	$\Delta T_3$	0.008	0.07
	$\Delta T_4$	0.008	0.072
	$\Delta T_5$	0.01	0.08
underestimation of (E)	$\Delta T_2$	0.1	0.07
	$\Delta T_3$	0.23	0.08
	$\Delta T_4$	0.2	0.08
	$\Delta T_5$	0.9	0.09
overestimation of $J_1$	$\Delta T_2$	2.68	0.35
	$\Delta T_3$	3.34	0.12
	$\Delta T_4$	3.02	0.12
	$\Delta T_5$	0.5	0.15
overestimation of $J_5$	$\Delta T_2$	2.3	0.09
	$\Delta T_3$	1.5	0.12
	$\Delta T_4$	1.67	0.23
	$\Delta T_5$	4.5	0.45

To quantitatively evaluate the controller's performance, the Integral of Squared Error (ISE) performance index is utilized. This evaluation is conducted using both exact parameters and underestimations of  $E$ ,  $J_1$  and  $J_2$ . The ISE values, calculated over the time range [0s–1s] for tension errors  $\Delta T_2$ ,  $\Delta T_3$ ,  $\Delta T_4$ , and  $T_5$  are provided in Table 1.

The obtained results clearly demonstrate the superior robustness of the proposed Integrator Backstepping controller when subjected to variations in system parameters, particularly the inertia of the rolls and the Young's modulus of the web. In contrast to the conventional PI controller, the IBSC consistently maintains better stability and accuracy, even under dynamic and uncertain operating conditions. This highlights its effectiveness in ensuring reliable control performance in real industrial environments.

## 5 Conclusion

This paper presented a robust nonlinear control strategy for the independent regulation of the master motor speed and mechanical tensions within a Multi-Drive Web Winding System (MDWWS). The control architecture is built upon the Integral Backstepping approach, which enables precise tracking of both speed and tension setpoints, even in the presence of significant parameter uncertainties, such as changes in the Young's modulus and the total inertias of the winder and unwinder units. The effectiveness of the proposed controller was thoroughly validated through both simulation (modeling and control in MATLAB/Simulink) and Processor-in-the-Loop (PIL) co-simulation using the TMDSCNCD28379D DSP board. Compared to the classical PI control strategy, the proposed solution exhibited superior performance and enhanced robustness under varying conditions.

Looking ahead, future research will focus on extending the validation process to include additional frameworks such as Hardware-in-the-Loop (HIL) testing. These studies will also explore implementation across diverse digital hardware platforms, including alternative DSPs, ASICs, and FPGAs, to further assess the scalability and real-time performance of the proposed control method.

## References

- Chen D., Wang M. (2006) Adaptive control of linear velocity and tension in winding system of dry plastic film laminating machine, in *2006 International Technology and Innovation Conference (ITIC 2006)*, Hangzhou, pp. 1919–1923. <https://doi.org/10.1049/cp:20061081>.
- Foti S., Testa A., De Caro S., Scimone T., Scelba G., Scarcella G. (2019) Multi-level open end windings multi-motor drives, *Energies* **12** (5), 5. <https://doi.org/10.3390/en12050861>.
- Al Sakka M., Geury T., El Baghdadi M., Dhaens M., Al Sakka M., Hegazy O. (2022) Review of fault tolerant multi-motor drive topologies for automotive applications, *Energies* **15**, 15, 15. <https://doi.org/10.3390/en15155529>.
- Rawat P., Liu S., Mahesh Kumar R., Singh N.K. (2023) Numerical investigation on the high-velocity impact resistance of textile reinforced composite mesh designs inspired by spider web, *J Text. Inst.* **115**, 1995–2010. <https://doi.org/10.1080/00405000.2023.2276863>.
- Kuznetsov B., Nikitina T., Bovdvi I.V. (2020) Structural-parametric synthesis of rolling mills multi-motor electric drives, *Electr. Eng. Electromechanics* **5**, 25–30. <https://doi.org/10.20998/2074-272X.2020.5.04>.
- Nishida T. (2013) Self-tuning PI control using adaptive PSO of a Web transport system with overlapping decentralized control, *Electr. Eng. Jpn.* **184**, 56–65.
- Wolfermann W. (1995) *Tension control of webs – A review of the problems and solutions in the present and future*. Accessed: Oct. 14, 2023. [Online]. Available: <https://shareok.org/handle/11244/321706>.
- Ponniah G., Zubair M., Doh Y., Choi K. (2013) Fuzzy decoupling to reduce propagation of tension disturbances in roll-to-roll system, *Int. J. Adv. Manuf. Technol.* **71**, 1–4. <https://doi.org/10.1007/s00170-013-5400-4>.
- Jee S., Kim S., Shin K.-H. (1999) Adaptive fuzzy control of tension variations due to the eccentric unwinding roll in multi-span web transport systems, in *Proceedings of the ASME 1999 International Mechanical Engineering Congress and Exposition. Dynamic Systems and Control*. Nashville, Tennessee, USA. November 14–19, The American Society of Mechanical Engineers, pp. 877–882. <https://doi.org/10.1115/IMECE1999-0119>.
- Wang C., Wang Y., Yang R., Lu H. (2004) Research on precision tension control system based on neural network, *Ind. Electron. IEEE Trans. On* **51**, 381–386. <https://doi.org/10.1109/TIE.2003.822096>.
- Angermann A., Aicher M., Schroder D. (2000) Time-optimal tension control for processing plants with continuous moving webs, in: *Proc. 35th Annual Meeting-IEEE Industry Applications Society, Rome, Rome*, pp. 3505–3511. <https://doi.org/10.1109/IAS.2000.882671>.
- Abjadi N.R., Soltani J., Askari J., Markadeh G.R.A. (2009) Nonlinear sliding-mode control of a multi-motor web-winding system without tension sensor, *IET Control Theory Amp. Appl.* **3**, 4, 419–427. <https://doi.org/10.1049/iet-cta.2008.0118>.
- Abjadi N.R., Askari J., Soltani J. (2008) Nonlinear decoupled control for multi-motors web winding system using the sliding-mode technique, in *IEEE International Conference on Networking Sensing and Control*, pp. 212–216. <https://doi.org/10.1109/ICNSC.2008.4525212>.
- Hou Y., Gao Z., Jiang F., Boulter B.T. (2001) Active disturbance rejection control for web tension regulation, in: *Proceedings of the 40th IEEE Conference on Decision and Control (Cat. No.01CH37228)*, vol. **5**, pp. 4974–4979. <https://doi.org/10.1109/CDC.2001.980997>.
- Zhang H., Xia H., Lu Y., Wu J., Zhang X., Wei Y. (2022) Tension control of a yarn winding system based on the nonlinear active disturbance-rejection control algorithm, *Text. Res. J.* **92**, 23–24, 5049–5065. <https://doi.org/10.1177/00405175221114658>.
- Xiong H., Lv Y., Cheng B., Nian X., Chu X. (2022) Motor model-based optimal robust guaranteed cost control for two-motor web-winding system, *Int. J. Control Autom. Syst.* **20**, 11, 3808–3821. <https://doi.org/10.1007/s12555-021-0293-8>.
- Baumgart M.D., Pao L.Y. (2003) Robust Lyapunov-based feedback control of nonlinear Web-winding systems, in *42nd IEEE International Conference on Decision and Control (IEEE Cat. No.03CH37475)*, Maui, HI, USA, Vol. **6**, pp. 6398–6405. <https://doi.org/10.1109/CDC.2003.1272347>.
- Baumgart M.D., Pao L.Y. (2003) A tension observer for nonlinear web-winding systems with air entrainment, in *Proceedings of the 2003 American Control Conference, June 2003, vol. 5*, pp. 4149–4154. <https://doi.org/10.1109/ACC.2003.1240486>.
- Nguyen V., Nguyen V., Tran T. (2019) Integrator-back-stepping based control for nonlinear roll-to-roll web dynamics, *J. Eng. Sci. Res.* **3**, 17–27. <https://doi.org/10.26666/rmp.jesr.2019.2.3>.
- El Haissouf M., Mustapha E.H., Abdellfattah B.-R. (2023) Processor in the loop experimentation of an integral back-stepping control strategy based torque observer for induction motor drive, *Int. Rev. Autom. Control IREACO* **16**, 92. <https://doi.org/10.15866/ireaco.v16i2.23063>.
- El Haissouf M., Mustapha E.H., Abdellfattah B.-R. (2021) Processor in the loop comparative study of indirect rotor field oriented control, direct self control, direct torque control and space vector modulation based direct torque control for induction motor drives, *Int. Rev. Model. Simul. IREMOS* **14**, 451. <https://doi.org/10.15866/iremos.v14i6.20997>.
- Chen Z., Zhang T., Zheng Y., Wong D., Deng Z. (2020) Fully decoupled control of the machine directional register in roll-to-roll printing system, *IEEE Trans. Ind. Electron.* **68**, 10007–10018. <https://doi.org/10.1109/TIE.2020.3029476>.
- Bensaid M., Abdellfattah B.-R., Mustapha E.H., Rached B. (2020) Effects of symmetrical voltage sags on two induction motors system coupled with an elastic web, in *2020 IEEE 2nd International Conference on Electronics, Control, Optimization and Computer Science (ICECOCS)*, Kenitra, Morocco, pp. 1–6. <https://doi.org/10.1109/ICECOCS50124.2020.9314298>.
- Bensaid M., Abdellfattah B.-R., Mustapha E.H. (2023) Management strategy to mitigate voltage sags effects of a multi-motors system using ADALINE algorithm and cascade sliding mode control, in *Int. J. Power Electron. Drive Syst.* **15**, 1. <https://doi.org/10.11591/ijpeds.v15.i1.pp239-250>.
- Bensaid M., Rached B., Mustapha E.H., Abdellfattah B.-R. (2020) Multi-drive electric vehicle system control using

backstepping strategy, in *2020 1st International Conference on Innovative Research in Applied Science, Engineering and Technology (IRASET)*, Meknes, Morocco, p. 6. <https://doi.org/10.1109/IRASET48871.2020.9092164>.

- 26 Mokhtari F., Sicard P. (2013) Decentralized control design using Integrator Backstepping for controlling web winding systems, in *IECON 2013 – 39th Annual Conference of the IEEE Industrial Electronics Society*, Vienna, Austria, pp. 3451–3456. <https://doi.org/10.1109/IECON.2013.6699683>.
- 27 Tran T., Newman B. (2015) Integrator-backstepping control design for nonlinear flight system dynamics, in *AIAA Guidance, Navigation, and Control Conference*. <https://doi.org/10.2514/6.2015-1321>.
- 28 Coban R. (2017) Dynamical adaptive integral backstepping variable structure controller design for uncertain systems and experimental application, *Int. J. Robust Nonlinear Control* **27**, 4522–4540. <https://doi.org/10.1002/rnc.3810>.
- 29 Bensaid M., Ba-Razzouk A., El Haroussi M., El Haisouf M. 2025. Processor in the loop of sliding mode control and observer utilizing the super twisting algorithm for mechanical tension in a multi-motor system, *Int. Rev. Electric. Eng.* **20**, 1, 9–19. <https://doi.org/10.15866/iree.v20i1.24653>.

## Appendix A: Parameters simulations.

**Table A1.** Winder system parameters and Control parameters.

Winder system parameters	
$L_{Bande}$	2 m
$S$	$2.75 \times 10^{-5} \text{ m}^2$
$E$	$1.6 \times 10^8 \text{ N/m}^2$
$J_1, J_5$	$1.25 \text{ kg m}^2$
$J_2, J_3, J_5$	$0.25 \text{ kg m}^2$
$r_1, r_5$	0.5 m
$r_2, r_3, r_5$	0.25 m
$f_1, f_2, f_3, f_4, f_5$	$0.004 \text{ N m}^{-1} \text{ S}$
$T_{ref}$	4 N
$V_{2ref}$	5 m/s
Control parameters	
$k_p$	200
$k_i$	5
$k_v$	0.5

## Appendix B

Specifications of development board TMDSCNCD28379D F28379D development kit for C2000™ Delfino MCU controlCARD™ [29].



Technical specifications of the TMDSDOCK28379D board:

- CPU: C28x.
- Memory: 1MB flash.
- 24 PWM and four 16bit or 12bit ADCs, sigma delta filter modules, capture interfaces, QEP interfaces, and serial connectivity.
- On-board emulator: XDS100 USB JTAG.